

See discussions, stats, and author profiles for this publication at: <https://www.researchgate.net/publication/341908741>

Geomechanical characterization of volcanic aggregates for paving construction applications and correlation with the rock properties

Article in *Transportation Geotechnics* · June 2020

DOI: 10.1016/j.trgeo.2020.100383

CITATIONS

0

READS

29

3 authors, including:



Cándida García-González

Universidad de Las Palmas de Gran Canaria

14 PUBLICATIONS 39 CITATIONS

[SEE PROFILE](#)



Miguel A. Franesqui

Universidad de Las Palmas de Gran Canaria

29 PUBLICATIONS 44 CITATIONS

[SEE PROFILE](#)

Some of the authors of this publication are also working on these related projects:



Sustainable self-healable perpetual asphalt pavements with volcanic aggregates using microwaves and additions of metallic wastes and nanoparticles (MW-VolcAsphalt). MINECO 2017 (Grant: BIA2017-86253-C2-R) [View project](#)



Sustainable development and production of warm-mix asphalt using recycled rubber from used tires and volcanic aggregates from the Canary Islands [VOLCANIC BC-WARM] [View project](#)

Journal Pre-proofs

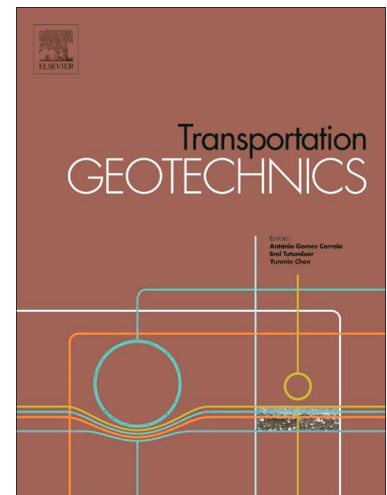
Geomechanical characterization of volcanic aggregates for paving construction applications and correlation with the rock properties

Cándida García-González, Jorge Yepes, Miguel A. Franesqui

PII: S2214-3912(20)30271-3
DOI: <https://doi.org/10.1016/j.trgeo.2020.100383>
Reference: TRGEO 100383

To appear in: *Transportation Geotechnics*

Received Date: 15 January 2020
Revised Date: 31 March 2020
Accepted Date: 2 April 2020

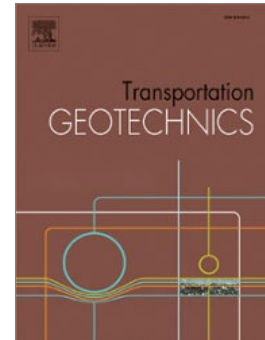


Please cite this article as: C. García-González, J. Yepes, M.A. Franesqui, Geomechanical characterization of volcanic aggregates for paving construction applications and correlation with the rock properties, *Transportation Geotechnics* (2020), doi: <https://doi.org/10.1016/j.trgeo.2020.100383>

This is a PDF file of an article that has undergone enhancements after acceptance, such as the addition of a cover page and metadata, and formatting for readability, but it is not yet the definitive version of record. This version will undergo additional copyediting, typesetting and review before it is published in its final form, but we are providing this version to give early visibility of the article. Please note that, during the production process, errors may be discovered which could affect the content, and all legal disclaimers that apply to the journal pertain.

García-González C, Yepes J, Franesqui MA (2020). Geomechanical characterization of volcanic aggregates for paving construction applications and correlation with the rock properties. *Transportation Geotechnics* 24: 100383. DOI: [10.1016/j.trgeo.2020.100383](https://doi.org/10.1016/j.trgeo.2020.100383)

To help you access and share this work, we have created a Share Link – a personalized URL providing **50 days' free access** to your article. **Anyone clicking on this link before August 01, 2020 will be taken directly to the final version of your article on ScienceDirect, which they are welcome to read or download. No sign up, registration or fees are required:**



<https://authors.elsevier.com/a/1bDgn7tVeY57Dv>

Geomechanical characterization of volcanic aggregates for paving construction applications and correlation with the rock properties

Cándida García-González ^a, Jorge Yepes ^b, Miguel A. Franesqui ^{a,*}

^a Grupo de Fabricación Integral y Avanzada – Departamento de Ingeniería Civil, Universidad de Las Palmas de Gran Canaria (ULPGC), Campus de Tafira, 35017 Las Palmas de Gran Canaria, Spain.

^b Departamento de Ingeniería Civil – IOCAG, Universidad de Las Palmas de Gran Canaria (ULPGC), Campus de Tafira, 35017 Las Palmas de Gran Canaria, Spain.

* Corresponding author. E-mail address: miguel.franesqui@ulpgc.es (M.A. Franesqui).

ABSTRACT

In volcanic terrains and in particular island regions, the aggregates come from the mechanical crushing of lava rocks and pyroclastic deposits. This study offers an experimental database of the geomechanical characteristics of different volcanic rock lithotypes and the aggregates obtained from these rocks. For this purpose, 971 aggregate samples and 643 rock samples of 11 different common volcanic lithotypes (including basalts, trachybasalts, trachytes, phonolites, ignimbrites and pyroclasts) were tested. These represent the majority of stone materials found in volcanic islands. Furthermore, correlations between the different properties of the aggregates (volumetric, geometric and mechanical properties) have been established, as well as between certain aggregate properties and the source rock. This allows an estimation of the foreseeable characteristics of the aggregates based on their origin. The results show that the aggregates from massive lithotypes provide superior resistance, partly due to their high density. These generally comply with the standard specifications although the particle shape may present an excessive flakiness index. However, the most abundant volcanic aggregates come from very porous rocks with a vesicular or scoriaceous structure, non-cubic particles, low resistance and high absorption, though they provide good drainage capacity. The high

statistic dispersion of the geomechanical properties is due to the different viscosity of the magmas, degrees of explosiveness of the volcanic eruption and random spatial distribution. Even the abundant vesicular and scoriaceous volcanic aggregates, generally considered as marginal materials, may offer adequate quality and properties for certain construction applications. In this sense, the use of these aggregates might contribute to the development of infrastructures in these regions and thus a sustainable utilization of this natural material.

Keywords: Volcanic aggregate; Volcanic rock; Massive volcanic aggregate; Vesicular volcanic aggregate; Scoriaceous volcanic aggregate; Pyroclastic aggregate; Pavement construction

Highlights:

- A characterization data base of the main volcanic aggregate lithotypes is provided for construction purposes.
- Utility of the simplified classification of volcanic aggregates into massive, vesicular and pyroclastic is confirmed.
- Relations among aggregate properties and between aggregate and rock properties are provided.
- Massive aggregates are recommended for road surface layers, vesicular for bases, and pyroclastic for permeable subgrades and fillings.

1. Introduction

Aggregates are fundamental in the construction industry. They constitute one of the most consumed products in the world and one of the four most important raw materials in world mining [1]. In volcanic regions, and especially on island territories, there are numerous environmental, technical and economic limitations and constraints regarding the exploitation of these aggregates. In this sense, it is fundamental to know the properties of all the natural aggregates in order to consider possible applications for different construction uses. The endogenous origin of volcanic territories determines a great variability and heterogeneity of existing

materials and their properties even within the same quarry or natural deposit. The spatial distribution of the different rocks is usually unpredictably irregular and discontinuous [2], either due to the wide diversity of possible lithologies (basalts, basanites, trachytes, phonolites, rhyolites, etc.), the different rock structure (massive, vesiculated, isotropic, anisotropic), the type of alteration (hydrothermal, diagenetic, weathering, thermal contact) or the type of eruption that produced the rocks quarried for aggregates (effusive, explosive). This accumulation of constraints explains the lack of scientific-technical literature regarding the implementation of volcanic aggregates [2].

The main objective of this study is to promote the diversification of usable volcanic material for construction implementation in these regions where resources and territory are limited as well as protected environmentally. Bearing this in mind, an exhaustive geomechanical characterization of the main lithotypes is offered for possible use in the construction of road or airport pavements, used as unbound granular material, or as an aggregate for asphalt mixture or for cement concrete. However, for this last application additional testing would be necessary: chemical stability, alkali-silica reactivity, long-term durability of unstable minerals. From these properties, characterized by the European test standard (EN), correlations between the different properties of volcanic aggregates and between these and the source rock are presented in order to infer expected properties as long as the origin is known. In this way, the following characteristics were determined: particle density (EN 1097-6), water absorption (EN 1097-6), flakiness index (EN 933-3), percentage of crushed and broken surfaces (EN 933-5), sand equivalent (EN 933-8), sand friability (UNE 83-115-89), resistance to wear (EN 1097-1) and resistance to fragmentation (EN 1097-2); as well as the following properties of the original rock: bulk density (EN 1936) and uniaxial compressive strength (EN 1926). Finally, a simplified classification of volcanic aggregates for engineering applications is confirmed which will simplify the complex geological classifications and thus allow technicians and operators take decisions regarding the possible construction uses of a certain type of volcanic aggregate.

1.1. Background

There are studies that support the use of certain volcanic aggregates in road engineering [1-6]. Some studies even analyse the use of certain marginal volcanic aggregates (ashes, scoriae, tuffs, basaltic lapilli) in cement concrete [7-11] and in asphalt mixtures [2,12-14] based on the hydraulic capacity, profitability and low

environmental impact [2,8]. However, the performance of the final product will always depend on the individual properties of each one of the component materials and the proportion in which they are used [15,16].

Up to now, characterization studies of volcanic materials have focused on determining the properties of certain aggregates after analysing the rock characteristics [17,18]. Generally speaking, when it comes to analysing the quality of an aggregate, a resistance characterization is carried out using tests such as Los-Angeles (LA) and Micro-Deval (M_{DE}) [6]. Other studies have sought a way to estimate the values of LA and M_{DE} coefficients by indirect tests that are quicker and more affordable [19,20-22]. Certain studies explored the way to deduce the LA coefficient from the results obtained with the Schmidt hammer, Point Load Test (PLT) and the porosity [22]. To this effect, this study analysed samples of igneous, metamorphic and sedimentary rocks with different LA coefficients (10-76%). The results showed a certain correlation between the LA coefficient and the I_s of the Point Load Test ($R^2 = 0.72$) and with the I_r results obtained by the Schmidt hammer ($R^2 = 0.62$). Furthermore, the correlations clearly improved separating the samples according to their porosity ($n < 1\%$ y $n > 1\%$). Further studies [20,21], that analysed different non volcanic lithotypes according to petrology, porosity and density, provided LA values from electric resistivity, density and porosity, accomplishing a good correlation between electric resistivity and the LA coefficient. In Ref. [19] the LA coefficient, the uniaxial compressive strength (UCS) and the bulk density (ρ_b) of various volcanic lithotypes from the Canary Islands (Spain) were correlated and it was concluded that it is possible to estimate the UCS from the LA and ρ_b ; these last properties can be obtained in an easier, quicker and more affordable manner.

1.2. Classification of volcanic materials

Among volcanic rocks it is possible to find a variety of materials with very different compositions (basaltic, basanitic, trachytic, phonolitic, tephritic or rhyolitic) and rock structure (lava flows, cemented or non-cemented pyroclasts, volcanic breccia, ignimbrites) [23,24]. A characterization of these rocks has been carried out with the works in Ref. [25-27] about lithotypes in the Canary Islands (Spain); an archipelago of volcanic origin situated in the Atlantic Ocean near the NW coast of Africa ($N28^\circ$, $W15^\circ30'$). In these works, a classification of volcanic rocks has been organized according to petrology and texture, and providing data concerning the geomechanical properties. These studies allowed the Regional Government of the Canary

Islands to publish a Guide for Geotechnical Studies in Building in the Canary Islands (GETCAN-011) [28], which classifies lava rocks by cohesion, lithology, texture and vesicularity; and the pyroclastic materials according to lithology, welding grade and particle size. However, although this rock classification may be a starting point to classify volcanic aggregates, it does not allow the deduction of properties for constructive applications of those aggregates obtained by fragmentation as the engineering characterization of aggregates has not been addressed in these studies. Consequently, up until now the main properties of the wide range of volcanic aggregates have not been characterized systematically. The lack of knowledge concerning their characteristics and the absence of specific technical regulations for their use, means that frequently works support additional costs due to the importation of materials or due to doubts regarding non-compliance with certain specifications [5].

A first step towards an engineering classification of volcanic aggregates for construction purposes has been established in Ref. [2], within the framework of a research of the utilization of marginal high-porosity volcanic aggregates in asphalt mixtures for pavements. The present study aims to present a thorough and systematic research that will allow the property characterization of different lithotypes of volcanic aggregates for practical construction applications as well as provide the correlations among these properties and with the source rock.

2. Experimental method

2.1. Materials

The volcanic aggregate samples (Fig. 1) and the volcanic rocks (Fig. 2) were obtained in different quarries and natural deposits around the different islands of the Canarian archipelago, and were initially gathered according to the classification in Ref. [27,28]. Most of the aggregate crushing plants in these quarries use jaw crushers for breaking rocks. A total of 971 aggregate samples (without any alteration) were tested. These were obtained using normalized sample procedures, including 3 different particle size fractions (10–20, 4–10 and 0–4 mm), and obtained from 22 localizations. These represent a total of 11 different lithotypes (4 different basalts, 1 trachybasalt, 1 trachyte, 1 phonolite, 2 ignimbrites and 2 pyroclasts; see Table 1). These samples allowed

1392 tests following the European standards (EN). In relation with the volcanic rock samples, cylindrical
 cores of different diameters were obtained for the UCS tests and bulk density tests according to the standards
 (EN). A total of 643 rock samples were tested with a total of 860 tests. The lithotypes mentioned in [Table 1](#)
 represent the majority of stone materials that may be found in volcanic territories.

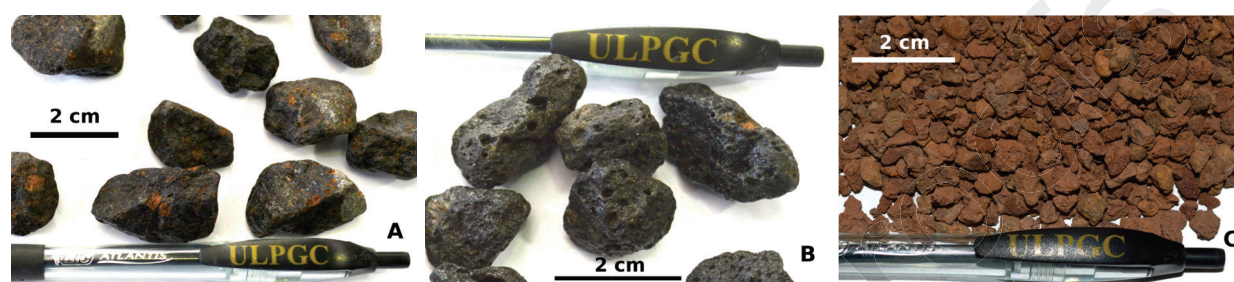


Fig. 1. Different lithotypes of volcanic aggregates: A) Massive black basalt (Gran-Canaria Island); B) Vesicular grey basalt (Fuerteventura Island); C) Example of pyroclasts: red ochre basaltic lapilli (Gran-Canaria Island).

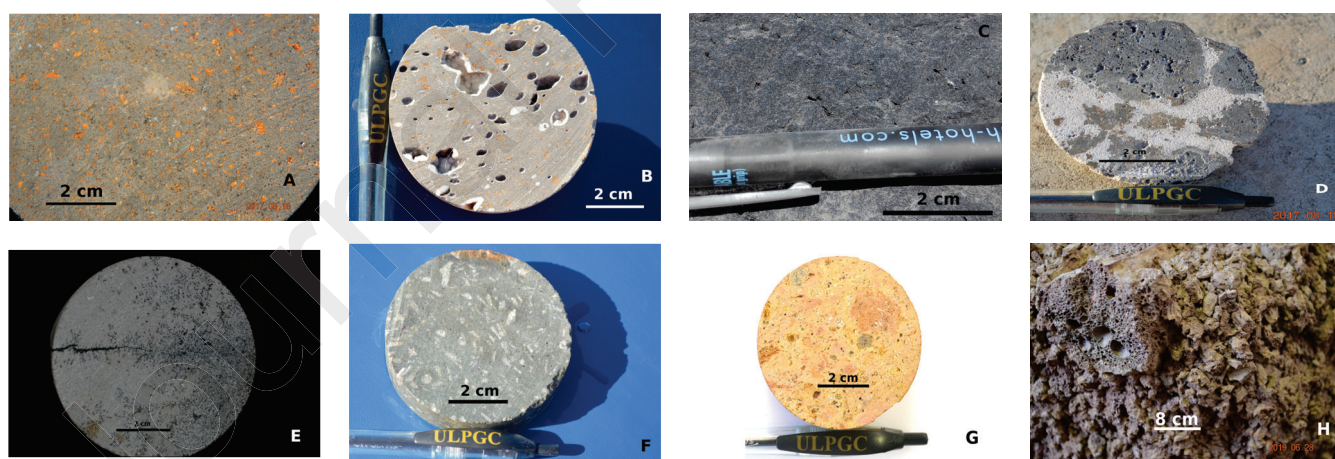


Fig. 2. Samples of volcanic rocks obtained from blocks and cylindrical cores: A) B-OP-M; B) B-OP-V; C) B-A-M; D) B-S; E) T; F) P; G) I-NW; H) L-NC (Red). (See description of each lithotype in [Table 1](#)).

Table 1

Engineering classification, description and recommended applications of the different volcanic lithotypes sampled in this research.

Volcanic lithotypes and subtypes			Abbrev.	Description [Geological age]	Location ^(X)	Recommended uses
Rocks	Basalt	Olivine-pyroxene basalt (Massive subtype) (<i>M</i>)	B-OP-M	Massive black basalt [Pleistocene]	28R459W3116N (La Isleta, Las Palmas, GC)	Asphalt mixture ^(*) (**), Cement concrete ^(*) , Road unbound granular base layer ^(*) (**)
				Massive black basalt [Pleistocene]	28R367W3152N (La Laguna, TF)	
				Massive weathered grey basalt [Miocene]	28R419W3098N (La Aldea de S. Nicolás, GC)	
		Olivine-pyroxene basalt (Vesicular subtype) (<i>V</i>)	B-OP-V	Vesicular grey basalt [Pleistocene]	28R459W3116N (La Isleta, Las Palmas, GC)	Road unbound granular base layer and subbase ^(**) , Subgrade ^(**) , Embankment ^(*) (**), Filling ^(*) (**)
				Vesicular grey basalt [Pleistocene]	28R608W3177N (Corralejo, La Oliva, FV)	
				Vesicular grey basalt [Pleistocene]	28R209W3075N (S. Andrés, Valverde, EH)	
				Vesicular black basalt [Pleistocene]	28R382W3153N (González Vilanova, TF)	
		Aphanitic basalt (Massive subtype) (<i>M</i>)	B-A-M	Massive grey basalt [Pleistocene]	28R354W3112N (La Cisnera, Arico, TF)	Asphalt mixture ^(*) (**), Cement concrete ^(*) , Road unbound granular base layer ^(*) (**)
		Scoriaceous basalt (<i>V</i>)	B-S	Scoriaceous ochre basalt [Pleistocene]	28R459W3116N (La Isleta, Las Palmas, GC)	Road unbound granular subbase ^(**) , Subgrade ^(**) , Embankment ^(**) , Filling ^(*)
		Trachybasalt (<i>M</i>)	TB	Light grey trachybasalt [Miocene]	28R356W3113N (GobCan, TF)	Asphalt mixture ^(**) , Cement concrete ^(*) , Road unbound granular base layer ^(**)
		Trachyte (<i>M</i>)	T	Beige trachyte [Miocene]	28R600W3163N (Tindaya, La Oliva, FV)	
	Phonolite	Massive phonolite (<i>M</i>)	P	Massive greenish phonolite [Late Miocene]	28R451W3075N (Juan Grande, S. Bartolomé, GC)	Asphalt mixture ^(*) (**), Cement concrete ^(*) , Road unbound granular base layer ^(*) (**)
				Phaneritic phonolite [Late Miocene]	28R433W3113N (Gáldar, GC)	
				Aphanitic phonolite [Late Miocene]	28R452W3105N (San Lorenzo, Las Palmas, GC)	
				Aphanitic phonolite [Late Miocene]	28R442W3073N (Fataga, S. Bartolomé, GC)	
		Welded ignimbrite (<i>V</i>)	I-W	Greenish ignimbrite [Late Miocene]	28R440W3079N (Ayagaures, S. Bartolomé, GC)	Cement concrete ^(*) (***), Road unbound granular base ^(*) , Ornamental stone ^(*)
Pyroclasts	Non-welded ignimbrite (<i>Py</i>)	I-NW		Beige non-welded ignimbrite (pumice) [Late Miocene]	28R434W3072N (Arguineguin, S. Bartolomé, GC)	Pozzolanic cement manufacture ^(*) , Non-structural lightweight concrete ^(*) (***), Ornamental stone ^(*)
	Non-cemented basaltic lapilli (<i>Py</i>)	L-NC (Black)		Black basaltic lapilli [Pleistocene]	28R459W3116N (La Isleta, Las Palmas, GC)	Permeable subbase and subgrade ^(**) , Permeable filling ^(*) (**), Non-structural lightweight concrete ^(*) (***), Gardening ^(*)
		L-NC (Red)		Red ochre basaltic lapilli [Pleistocene]	28R459W3116N (La Isleta, Las Palmas, GC)	

(*M*) Massive class; (*V*) Vesicular class; (*Py*) Pyroclastic class; (TF) Tenerife Island; (GC) Gran-Canaria Island; (FV) Fuerteventura Island; (EH) El-Hierro Island; (*) Practical experience by paving construction industry in the Canary Islands; (**) Recommended application according to results of this study; (***) For cement concrete it is necessary to limit the alkali-silica reactivity; (X) UTM coordinates are accurate to 1 km.

2.2. Instruments

To characterize the main volumetric, shape and resistance properties of the different aggregate fractions, the following laboratory equipment was utilized: a) standard testing sieves according to EN 933-2 and bar sieves (EN 933-3); b) balances, resolution ± 0.1 g and accuracy $\pm 0.1\%$; c) laboratory ovens (Matest), capacity 100 litres, natural convection and thermostatic control up to 250 °C, resolution ± 0.1 °C and accuracy ± 1.0 °C; d) glass pycnometers, capacity 1.3 litres, previously calibrated (0.001327 m^3); e) Los-Angeles drum machine (Mecacisa), 32 ± 1 min, with 11 steel balls of 440 g; f) Micro-Deval rotary 160 machine (Matest), 100 ± 5 rad/min, with steel balls $\varnothing 10$ mm; g) laboratory ovens (Matest), capacity 100 litres, natural convection and thermostatic control up to 250 °C, resolution ± 0.1 °C and accuracy ± 1.0 °C; h) universal testing machine (10 ton) with 1000 kN capacity.

2.3. Laboratory tests

In order to characterize the aggregates, the petrological nature, the inherent properties (density, porosity, particle shape and angularity) and the mechanical properties (resistance to fragmentation and to wear) were taken into account. As for the rocks, these were characterized by density and resistance properties.

Tests were performed on the different rock cores and on each one of the three fractions of the aggregate samples: coarse fraction (10-20 mm), medium fraction (4-10 mm) and fine fraction (0-4 mm), with the aim of observing performance differences among particle size fractions and correlating rock-aggregate properties. The values obtained were assessed according to different road specifications [29-31].

The density of the dry particles (ρ_{rd}) and the density of the saturated particles with the dry surface (ρ_{ssd}) were measured for determining the apparent particle density (ρ_a) by the pycnometer method (EN 1097-6) and the water absorption after 24 hours (WA_{24}) (EN 1097-6), according to Eq. (1) a (4) in Table 2.

To obtain the flakiness index (FI) specified sieves were used according to EN 933-3 and Eq. (5). For the determination of the percentages of crushed and broken surfaces $C_{(c,r,tc,tr)}$ (EN 933-5) coarse fraction was used, and the crushed particles (M_c), rounded particles (M_r), totally crushed particles (M_{tc}) and totally rounded particles (M_{tr}) were manually separated. Eq. (6) was used for the calculations of these indexes.

To obtain the sand equivalent (SE_{10}) the fraction grading 0-2 mm was tested according to standard EN 933-8 and calculations according to Eq. (7).

In order to determine the resistance to fragmentation by the Los-Angeles (LA) test (according to EN 1097-2), 5 kg of coarse fraction (10-20 mm) aggregate were mixed with the abrasive load (422 ± 22 g), according to the standard proportion (40% aggregate 10-12.5 mm; 60% aggregate 12.5-16 mm; 11 steel balls \varnothing 45-49 mm). For the medium fraction (4-10 mm), alternative proportions were employed (4-6.3 mm and 4-8 mm), according to standard (EN 1097-2). The drum speed was 31-33 rpm during 500 revolutions of the test. The LA coefficient was calculated according to Eq. (8).

To determine the resistance to wear in the Micro-Deval (M_{DE}) device (EN 1097-1), 500 g of aggregate were mixed with the abrasive load following standard proportions (40% aggregate 10-12.5 mm; 60% aggregate 12.5-16 mm; steel balls \varnothing 10 mm, and 2.5 ± 0.05 L of water). For the medium fraction (4-10 mm), alternative proportions were used (4-6.3 mm and 4-8 mm), according to standard (EN 1097-1). During the test, the drums spun 12000 ± 10 spins at 100 ± 5 rpm. The M_{DE} coefficient was calculated according to Eq. (9).

To determine the sand friability (SF) using the Micro-Deval equipment (UNE 83-115-89), 500 g of aggregate 1-2 mm were mixed with the abrasive load (2500 ± 4 g) according to standard proportions (9 steel balls \varnothing 30 mm and 110 g; 21 balls \varnothing 18 mm and 25 g; 246 balls \varnothing 10 mm and 4 g, and 2.5 L of water). During the test, the drums spun 1500 spins at 100 ± 5 rpm. The SF coefficient was calculated according to Eq. (10).

The bulk density (ρ_b) of the rocks was calculated using a hydrostatic scale (EN 1936) and Eq. (11). The resistance to uniaxial compressive strength (UCS) of the rocks (EN 1926) was determined by testing the cylindrical specimens in the hydraulic press with a minimum of 5 specimens for each rock sample, according to test Standard (ratio length/diameter of the sample 2.5, and load speed 0.5-1 MPa/s) and Eq. (12).

Table 2

Expressions used to calculate the different properties of aggregates and rocks, according to laboratory test European standards (EN).

Properties	Laboratory test	Equation	Test measurements
Aggregate volumetric properties	Apparent particle density	$\rho_a = \rho_w \frac{M_4}{M_4 - (M_2 - M_3)}$	(Eq. 1) (M ₁) saturated aggregate mass with dry surface, in g;
	Density of the dry particles	$\rho_{rd} = \rho_w \frac{M_4}{M_1 - (M_2 - M_3)}$	(Eq. 2) (M ₂) pycnometer mass with the saturated aggregate, in g;
	Density of the saturated particles with the dry surface	$\rho_{ssd} = \rho_w \frac{M_1}{M_1 - (M_2 - M_3)}$	(Eq. 3) (M ₃) pycnometer mass full of water, in g;
	Water absorption after 24 hours	$WA_{24} = \frac{M_1 - M_4}{M_4} \cdot 100$	(Eq. 4) (M ₄) dry aggregate mass, in g; (ρ_w) water density at the temperature when weighting M ₂ , in g/cm ³ .
Aggregate geometric properties	Flakiness index	$FI = \frac{M_2}{M_1} \cdot 100$	(Eq. 5) (M ₂) total mass of the particles passing through the bar sieve; (M ₁) total mass tested.
	Percentages of crushed and broken surfaces	$C_{(c,r,lc,tr)} = \frac{M_{(c,r,lc,tr)}}{M_1} \cdot 100$	(Eq. 6) M _(c,r,lc,tr) mass of each group of particles; (M _c) particles with more than 50% of crushed surfaces; (M _r) particles with more than 50% of rounded surfaces; (M _{lc}) particles with more than 90% of crushed surfaces; (M _{tr}) particles totally rounded; (M ₁) total mass tested.
Aggregate impurities	Sand equivalent	$SE_{10} = \frac{h_2}{h_1} \cdot 100$	(Eq. 7) (h ₁) total suspension height with respect to the base; (h ₂) sediment height.
Aggregate mechanical performance properties	Los-Angeles coefficient	$LA = \frac{5000 - m}{50}$	(Eq. 8) (m) retained mass by sieve #1.6 mm, in g after the test.
	Micro-Deval coefficient	$M_{DE} = \frac{500 - m}{5}$	(Eq. 9)
	Sand friability	$SF = \frac{m}{M} \cdot 100$	(Eq. 10) (M) initial sample mass in g; (m) final mass of particles Ø < 0.05 mm, in g.
Rock properties	Bulk density	$\rho_b = \rho_w \frac{m_d}{m_s - m_h}$	(Eq. 11) (m _d) mass of the dry rock sample (core), in g; (m _s) saturated mass of the rock sample, in g; (m _h) submerged mass, in g; (ρ_w) water density, in g/cm ³ .
	Uniaxial compressive strength	$UCS = \frac{F}{S}$	(Eq. 12) (F) Total failure load, in N; (S) Cross section area of the sample, in mm ² .

3. RESULTS

Table 3 shows the results of the average values of each property for the samples of different aggregate fractions from the same site or quarry.

Table 3

Average values for each aggregate fraction of the different properties in the samples of the different lithotypes of volcanic aggregates and locations.

Lithotype (See Table 1)	Location	Fraction 10-20 mm									Fraction 4-10 mm							Fraction 0-4 mm		
		ρ_a	ρ_{rd}	ρ_{ssd}	WA ₂₄	FI	Cc	LA	M _{DE}		ρ_a	ρ_{rd}	ρ_{ssd}	WA ₂₄	FI	LA	M _{DE}	ρ_a	SF	SE ₁₀
B-OP-M	GC (Las Palmas)	3.10	2.98	3.06	1.90	11	90	15	21		3.03	2.85	2.94	2.89	21	19	23	2.87	27	72
B-OP-M	TF (La Laguna)	2.95	2.66	2.76	3.64	9	67	17			3.12	2.81	2.83	7.18		36				
B-OP-M	TF (Peñate Caballero)		2.75		2.57	19	92	18				2.74		2.96	21	19				82
B-OP-M	TF (González Vilanova)		2.69	2.72	2.22	11		12				2.55	2.62	2.93				2.94		
B-OP-M	GC (La Aldea)	2.77	2.58	2.70	4.73			32	54		2.75	2.43	2.62	7.58	7		65	2.70		
B-OP-V	GC (Las Palmas)	2.90	2.58	2.70	4.47	4	44	31	15		2.94	2.65	2.77	4.52	3	35	31	2.83	26	65
B-OP-V	GC (Las Palmas)	2.97	2.61	2.74	5.04	9	68	37	28											
B-OP-V	GC (Las Palmas)	2.87	2.52	2.67	6.01	4	53	32	12											
B-OP-V	FV (Corralejo)	2.76	2.21	2.42	9.20	2	62	20	14		2.87	2.28	2.49	9.16	8	21	16	2.07	74	88
B-OP-V	EH (S. Andrés)	2.96	2.47	2.63	6.39	5	54	20			2.83	2.18	2.42	11.13	8					68
B-OP-V	TF (González Vilanova)		2.55		3.59	14		18												
B-A-M	TF (Arico)	2.54	2.50	2.40	2.85	7	84	18			2.79	2.60	2.59	3.06	8	16		2.99		75
B-S	GC (Las Palmas)	2.69	2.01	2.27	12.99	3	52	42	34		2.95	2.38	2.58	8.44	2	54	57	3.01	17	97
TB	TF (GobCan)	2.83	2.66	2.72	2.37		77	21										2.93		
T	FV (La Oliva)	2.62	2.39	2.48	3.46		82	24										2.70		60
P	GC (Juan Grande)	2.66	2.57	2.60	1.10	20	61	11	15		2.71	2.52	2.59	2.67	25			2.67		77
P	GC (Gáldar)	2.66	2.50	2.55	1.95	27	62	22	25		2.65	2.41	2.42	2.13	30	30		2.61		84
P	GC (San Lorenzo)	2.67	2.58	2.59	1.24	22		23	16		2.48	2.70	2.56	3.40		23		2.60		
P	GC (Fataga)	2.61	2.57	2.59	1.60	13	79	12	6		2.65	2.52	2.57	2.73	20	16	10	2.62	24	76
I-NW (Pumice)	GC (S. Bartolomé)	2.05	1.34	1.70	27.60			35	74		2.30	1.38	1.80	30.62		35	78	2.22	55	
L-NC (Black)	GC (Las Palmas)	2.13	1.41	1.75	23.88	4	72	37	26		2.44	1.45	1.87	28.96	2	32	57	2.69	15	93
L-NC (Red)	GC (Las Palmas)	1.99	1.43	1.72	20.29	3	65	47	29		1.96	1.25	1.62	29.97	2	31	63	2.41	12	99

(ρ_a) Particle density [EN 1097-6] in g/cm³; (ρ_{rd}) Particle density [dry] in g/cm³; (ρ_{ssd}) Density of the saturated particles with the dry surface, in g/cm³; (WA₂₄) Water absorption of particles after 24 h [EN 1097-6] in %; (FI) Flakiness index [EN 933-3] in %; (Cc) Percentage of particles with more than 50% of their surface crushed or broken [EN 933-5]; (LA) Los-Angeles coefficient [EN 1097-2]; (M_{DE}) Micro-Deval coefficient [EN 1097-1]; (SF) Sand Friability [UNE 83-115-89] in %; (SE₁₀) Sand Equivalent [EN 933-8] in %; (TF) Tenerife Island; (GC) Gran-Canaria Island; (FV) Fuerteventura Island; (EH) El-Hierro Island.

In order to provide certain reference values of the volcanic aggregate properties that might have a more universal application and thus serve as a guide in the construction sectors, the previous results were averaged for the samples of the same lithotype with the three grading fractions. These results are shown in Table 4.

Furthermore, in order to consider the decomposition of the matrix rock, certain lithological groups were assigned a weathering grade according to ISMR (1981) classification [32], where: grade (I) Unweathered rock mass (no visible sign of decomposition or discoloration); grade (II) Slightly weathered rock mass (slight discoloration inwards from open fractures; discontinuity may be somewhat weaker externally than in its fresh condition); and grade (III) Moderately weathered rock mass (less than half of the rock mass is decomposed to a soil; weaker minerals decomposed; strength somewhat less than fresh rock but cores cannot be broken by hand or scraped by knife).

Table 4

Reference values for construction purposes of the main characteristics of the different volcanic aggregate lithotypes studied in this research. Results averaged for all the fractions in each lithotype.

Lithotype (See Table 1)	ρ_{rd} (g/cm ³)			WA ₂₄ (%)			FI (%)			Cc (%)			M _{DE}			LA			SF (%)			SE ₁₀ (%)		
	N	Mean	Sd	N	Mean	Sd	N	Mean	Sd	N	Mean	Sd	N	Mean	Sd	N	Mean	Sd	N	Mean	Sd	N	Mean	Sd
B-OP-M (I)	52	2.80	0.20	62	2.88	1.68	22	16	7	16	87	8	16	22	2	34	17	6	11	28	6	14	75	13
B-OP-M (III)	24	2.49	0.09	24	6.39	1.63	3	7	1				28	60	7	11	32	4						
B-OP-V (I)	59	2.45	0.42	59	8.7	10.9	32	6	4	26	56	15	43	20	8	28	28	7	17	49	26	22	76	12
B-A-M (I)	21	2.56	0.20	12	3.54	2.69	17	7	2	13	83	20				6	14	7			8	75	7	
B-S (III)	30	2.39	0.39	30	9	5	10	3	1	5	52	21	16	45	12	9	46	7	8	17	3	10	97	1
TB	2	2.68	0.02	2	2.72	0.49										2	33	16						
T	3	2.50	0.12	3	2.50	0.85				2	82	0	1	77		4	32	12						
P	69	2.55	0.11	71	2	1	40	21	8	12	72	13	22	11	6	34	18	7	8	24	1	20	77	8
I-W (greenish)																4	36	9						
I-NW (Pumice)	7	1.42	0.11	7	28	5							14	76	3	10	39	9	6	55	6			
L-NC (Black)	45	1.48	0.38	41	20	9	10	3	1	5	65	21	16	46	17	8	39	9	8	12	1	10	99	2
L-NC (Red)	27	1.79	0.52	27	20	10	9	3	2	4	72	10	16	42	16	7	35	3	8	15	1	10	93	4
Total number of samples tested	339			338			143			83		172			157			66			94			

(ρ_{rd}) Particle density [dry]; (WA₂₄) Water absorption of particles after 24 h [EN 1097-6]; (FI) Flakiness index [EN 933-3]; (Cc) Percentage of particles with more than 50% of their surface crushed or broken [EN 933-5]; (M_{DE}) Micro-Deval coefficient [EN 1097-1]; (LA) Los-Angeles coefficient [EN 1097-2]; (SF) Sand Friability [UNE 83-115-89]; (SE₁₀) Sand Equivalent [EN 933-8]; (N) Number of samples tested; (Mean) Average value; (Sd) Standard deviation; (I, II, III) Weathering grade according to ISMR (1981) [32].

Table 5 summarises the reference values of the tested properties in the cores from different volcanic rock lithotypes, including the weathering grades.

Table 5

Reference values of the main characteristics of the different volcanic rock lithotypes studied in this research. Results averaged for all the samples in each lithotype.

Lithotype (See Table 1)	ρ_b (g/cm ³)			UCS (MPa)		
	N	Mean	Sd	N	Mean	Sd
B-OP-M (I)	86	3,16	0,07	20	124,67	32,75
B-OP-M (III)	44	2,72	0,11	7	39,21	18,78
B-OP-V (I)	105	2,58	0.16	29	36.63	30.06
B-OP-V (II)	42	2.26	0.21	5	8.70	2.19
B-A-M (I)	8	2.96	0.11	7	110.57	55.95
B-A-M (II)	2	2.64	0.32	1	130.27	-
B-A-V (II)	3	2.42	0.08	2	26.76	1.43
B-PL-M (I)	2	2.97	0.07	1	122.71	-
B-S (I)				2	65.08	80.92
B-S (III)	34	2.39	0.09	10	18.30	6.63
TB	2	2.21	0.44	2	60.98	57.06
T	3	2.35	0.06	3	79.49	38.82
P	6	2.37	0.23	24	126.51	69.08
I-W (greenish)	9	2.49	0.06	13	52.71	25.86
I-W (beige)	3	2.19	0.12	3	19.62	6.50
I-W (red ochre)	23	1.88	0.20	3	7.67	3.79
I-W (green)	58	2.36	0.02	14	81.06	25.55
I-NW (orange) (II)	42	2.02	0.03	34	20.27	6.69
I-NW (Pumice)	3	1.52	0.46	7	18.51	21.97
L-C (Black)	102	1.64	0.28	14	20.76	7.12
L-C (Red)	66	1.44	0.05	16	6.84	1.76
Total number of samples tested	643			217		

(ρ_b) Bulk density [EN-1936]; (UCS) Uniaxial compression strength [EN-1926]; (N) Number of samples tested; (Mean) Average value; (Sd) Standard deviation; (I, II, III) Weathering grade according to ISMR (1981) [32].

4. DISCUSSION

Prior to the establishment of correlations among the different aggregate properties, each one has been correlated with the density of each grading fraction separately. In this way, the influence due to the density-porosity change among fractions has been assessed. As a reference the particle density [dry] (ρ_{rd}) was used, except for the finest fraction (0-4 mm); in this case the apparent particle density (ρ_a) was employed. In this manner, the measurement of the density of the saturated particles with the dry surface (ρ_{ssd}) was avoided when using the pycnometer method for 0-4 mm fraction, as this determination could be subjective due to the small size of the particles.

4.1. Aggregate volumetric properties

Fig. 3 shows the average values of the apparent particle density (ρ_a) and the particle density [dry] (ρ_{rd}) depending on the lithotype; these values have been classified by increasing ρ_{rd} . The differences between both densities are significant in the case of the pyroclastic (L-NC, I-NW) and vesicular aggregates (B-S, B-OP-V), although in all cases ρ_a was above ρ_{rd} . This difference is attributable to the water absorption percentage after 24 hours (WA_{24}), very low in the case of the aggregates obtained from massive lava (P, B-A-M, TB, B-OP-M) but very high in the case of pyroclastic and vesicular aggregates.

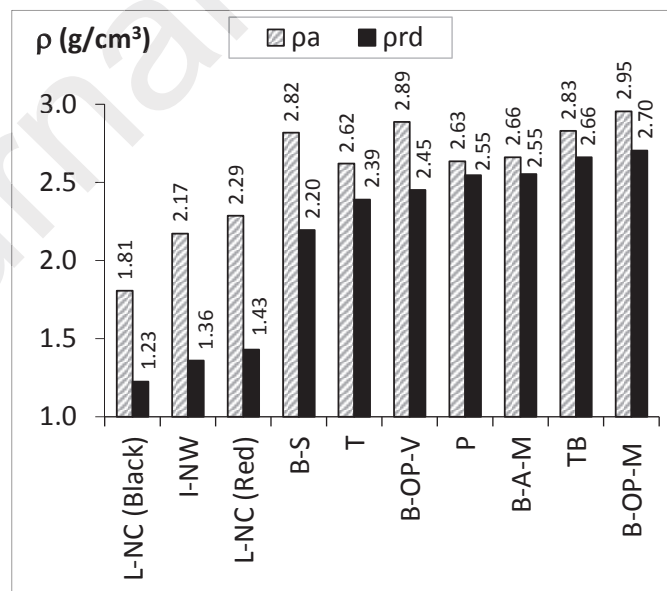
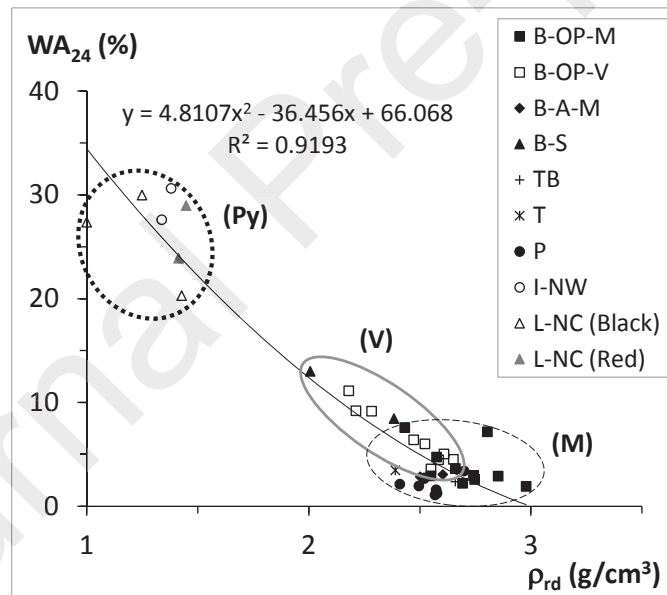


Fig. 3. Apparent particle density (ρ_a) and particle density [dry] (ρ_{rd}). Reference values for the different lithotypes of volcanic aggregates.

249

250 Fig. 4 shows the WA_{24} , that can be assimilated to the porosity of the aggregate, with regard to the ρ_{rd} . In this
 251 graph, three large lithological groups can be distinguished as mentioned before in Ref. [2]: a) pyroclastic
 252 aggregates, of low density and very high porosity; b) vesicular aggregates, situated in the intermediate zone
 253 (medium-high density and medium-high porosity); and c) massive aggregates of high density and low
 254 porosity. As the ρ_{rd} increases the WA_{24} becomes lower. The non-linear regression model is good ($R^2 = 0.92$)
 255 despite the fact that the results show broad statistical dispersion in the high part of the fitting line. This broad
 256 spread is related to the heterogeneity of the materials under study and particularly the pyroclasts whose
 257 variability in WA_{24} (Standard deviation, $Sd = 9-10\%$) is determined by the high content of voids, the
 258 polymictic character and the chaotic structure with a cluster like form.

259



260

261 **Fig. 4.** Water absorption (WA_{24}) vs. particle density [dry] (ρ_{rd}) of the aggregate. (M)
 262 Massive lithotypes; (V) Vesicular coherent lithotypes; (Py) Pyroclastic lithotypes.

263

264 4.2. Aggregate geometric properties

265 Fig. 5 analyses the relation between the aggregate particle density [dry] (ρ_{rd}) and its geometrical properties:
 266 flakiness index (FI) and percentage of crushed and broken surfaces (Cc). Higher values of FI ($FI > 20$) denote

materials with a high proportion of flaky particles (Fig. 5.A). Although it is not possible to establish a tendency line due to the heterogeneity of the volcanic material, certain lithotypes —especially the pyroclastic, scoriaceous and vesicular lithotypes— do comply with road technical specifications [29-31]. As for the low values of Cc (Fig. 5.B), these denote a lower content of crushed particles and a higher content of rounded particles, and do not comply with specifications. In this sense, the presence of material with a high FI will favour the appearance of fractures and settlings both in filling structures (embankments, unbound granular layers) as well as in asphalt mixtures and cement concrete structures. This fact is associated with local structure collapse and is due to the fact that the particles with this flake-like shape break more easily during compaction and even under traffic loads. Consequently, the grading modifications of the aggregate size, together with the dynamic traffic loads could possibly cause vertical settling in the road structure and increase compactability.

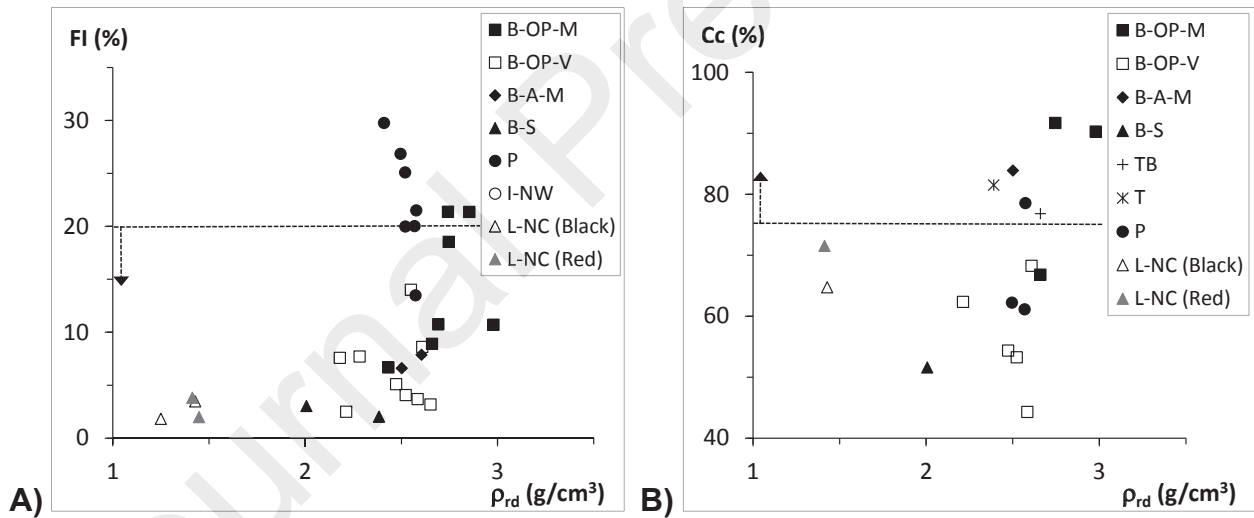


Fig. 5. Aggregate geometric properties vs. particle density [dry] (ρ_{rd}): A) Flakiness index (FI); B) Percentages of crushed and broken surfaces (Cc). (The horizontal dotted lines represent limit values specified for road pavement construction [29]).

Fig. 5.A shows how the less dense aggregates such as pyroclastic (L-NC), scoriaceous (B-S) and vesicular (B-OP-V), present a lower content of particles with flaky shape (FI) compared to the massive (P, B-OP-M). Fig. 5.B shows how the pyroclastic and vesicular aggregates have a content of crushed particles (Cc) below the

recommended limits. Some examples of these limits defined by different road specifications are as follows: USA (FHWA): $FI \leq 10\%$, $Cc \geq 75-90\%$ [30]; UK: $FI \leq 25\%$ [31]; Spain: $FI \leq 20-30\%$, $Cc \geq 70-100\%$, depending on the heavy traffic category [29]).

These two characteristics (FI and Cc) are related to the structure of the source rock; that is the spatial distribution of its components (minerals and voids). The massive lithotypes come from effusive volcanic eruptions and have weak parallel planes. This anisotropic structure determines the aggregate angularity. By contrast, the pyroclastic and vesicular lithotypes come from explosive eruptions characterized by a superior abundance of gases [33]. These conditions give the fragments an isotropic structure and condition the cracking geometry during the rock grinding process. The surfaces with a higher percentage of pores are the first to break. This determines the formation of warped fracture surfaces, and consequently rounded particles. The degree of roundness is directly related to the percentage of gaseous fraction in the lava. This is the case of non-welded ignimbrites (I-NW) and pyroclasts (L-NC).

Previous studies [34] have also shown that aggregate shape properties are affected by the type of crusher used in the aggregate crushing plants. In this sense, since most of the samples were obtained using jaw crushers, this may explain the high values of FI obtained for some hard rock lithotypes such as phonolites (P) or massive basalts (B-OP-M).

Fig. 6 allows the analysis of the sand content of the fine fraction (0-4 mm). This graph compares the apparent particle density (ρ_a) of the fine aggregate to the sand equivalent (SE_{10}). The specified limits defined by different road specifications are: USA-FHWA: $SE_{10} \geq 45\%$ [30]; Spain: $SE_{10} > 45-55\%$ [29]).

In general terms, the percentage of the finest particles $\# < 0.08$ mm (inverse of SE_{10}) increases with the massive character of the material. A priori, a higher proportion of the finest particles would be expected in the more porous materials, but the results show the opposite. This may be explained because the pyroclasts and the scoriaceous aggregates tested (L-NC, B-S) are natural aggregates that have not undergone mechanical grinding and would confirm the findings at the quarries: grinding generates waste dust that gathers in the fine fraction. Furthermore, the percentage of the finest fraction may be enriched due to winds at the quarry. These

observations suggest that SE_{10} also depends on the aggregate production more than the intrinsic properties of the source rock.

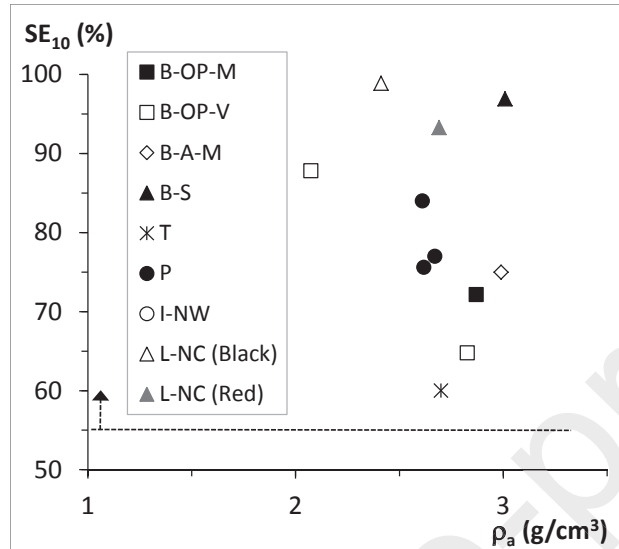


Fig. 6. Sand equivalent (SE_{10}) vs. apparent particle density (ρ_a) of the aggregate. (The horizontal dotted line represents a specified limit for road pavement construction [29]).

4.3. Aggregate mechanical performance properties

The aggregate resistance analysis focused on the parameters that quantify the wear caused by fragmentation and abrasion: Los-Angeles (LA), Micro-Deval (M_{DE}) and sand friability (SF) coefficients. Indexes above 50 correspond to bad quality aggregates which are not suited for road paving. Coefficients below 20 or 30 correspond to resistant aggregates suitable for any application and in particular for bituminous surfaces that support heavy traffic [29-31].

Fig. 7.A shows the relation between the particle density [dry] (ρ_{rd}) of the aggregate and the resistance to fragmentation, expressed by the LA coefficient of the aggregate coarsest fractions (10-20 y 4-10 mm). Fig. 7.B presents the relation between (ρ_{rd}) and the resistance to wear, expressed by the M_{DE} coefficient.

It may be noticed that LA and M_{DE} decrease as ρ_{rd} increases. In both cases, the aggregates from massive materials (B-OP-M, P) offer similar values, except for the samples obtained from the more weathered rocks

(B-OP-M (III)), which provide results similar to those obtained from pyroclastic materials. The values of the massive aggregates (B-OP-M, B-A-M, P) comply with road specifications. The recommended limits defined by different road technical specifications are as follows: USA (FHWA): $LA \leq 35$ [30]; UK: $LA \leq 30-35$; [31]; Spain: $LA \leq 20-25$; $M_{DE} \leq 20-25$, depending on the heavy traffic category and type of road layer [29]).

Regarding the scoriaceous and pyroclastic aggregates (B-S, I-NW, L-NC), these offer highly disperse results with very high LA and M_{DE} coefficients in some cases (Table 4). The aggregates from vesicular lava (B-OP-V) can be placed in an intermediate position. They present some dispersion in the results but do comply with technical specifications in certain cases. This suggests that the mechanical behaviour of the B-OP-V would improve with the addition of polymers such as rubber as these will fill the pores and lend consistency to the material, as has been demonstrated in a previous study [2]. In this sense, powder additions should be used so that the polymer grading is smaller than the average pore size of the aggregate (2-8 mm).

These results are in accordance with the satisfactory statistical correlation offered by LA coefficient with some aggregate properties (water absorption, density and porosity) previously reported by some reference [35].

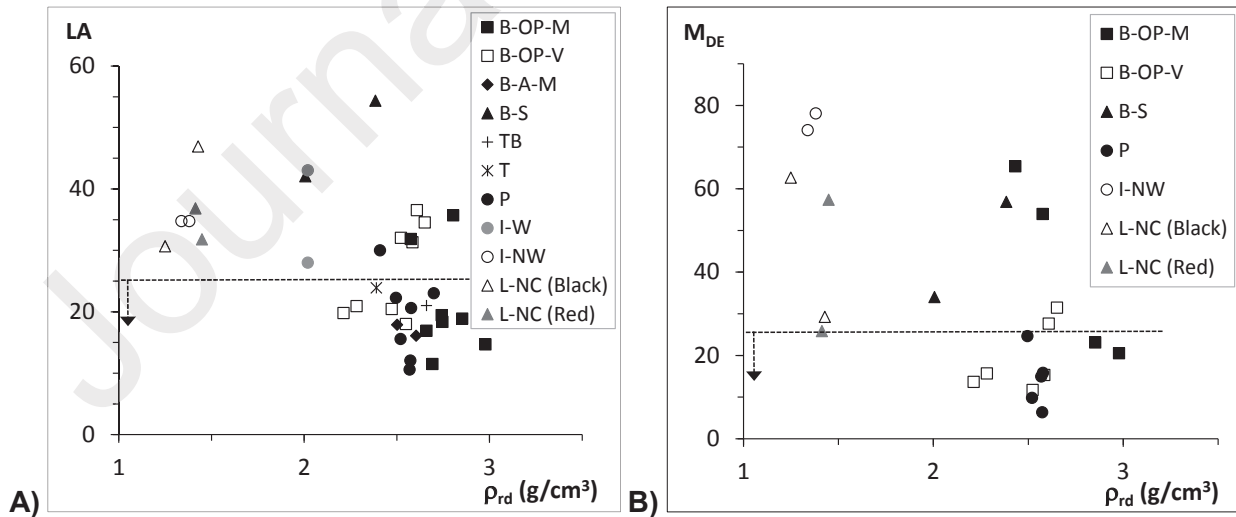


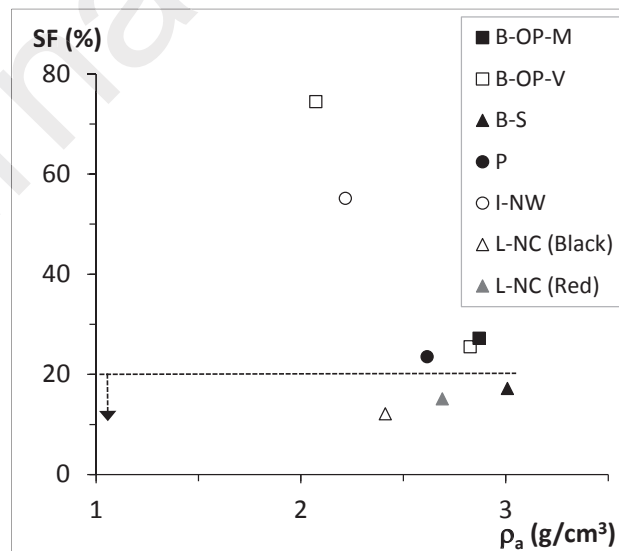
Fig. 7. Aggregate strength properties vs. particle density [dry] (ρ_{rd}): A) Los-Angeles coefficient (LA); B) Micro-Deval coefficient (M_{DE}). (The horizontal dotted lines represent limit values specified for road pavement construction [29]).

349

350 Determination of the resistance to fragmentation of the fine aggregate (0-4 mm) was based on the sand
 351 friability coefficient (SF). Fig. 8 shows how the SF coefficient decreases as the apparent particle density (ρ_a)
 352 of the aggregate increases. In this figure a limit value defined by certain road specifications is also shown (SF
 353 $< 20\%$ [29]).

354 The massive materials (B-OP-M, P) offer similar values (SF > 20), meanwhile the vesicular materials (B-OP-
 355 V) present a high level of dispersion (Table 4). Generally speaking, friability depends on the lithotype
 356 mineralogy and do not on the porosity as observed in the rest of properties. Materials with a higher iron
 357 content seems to show a higher resistance to wear. Nevertheless, the pyroclasts (L-NC) and the aggregates
 358 obtained from scoriaceous basaltic lava (B-S) offer a much lower SF than expected. This may be explained by
 359 the low density and floatability of the lapilli and thus, during the spinning process in the test, the lighter
 360 particles would be in suspension. This would reduce the time that the aggregate remains at the bottom of the
 361 drum, and consequently reduce the period of contact between the aggregate and the abrasive load during the
 362 test, and as a result resistance to friability would be higher.

363



364

365 **Fig. 8.** Sand friability (SF) vs. apparent particle density (ρ_a) of the aggregate. (The
 366 horizontal dotted line represents a specified limit for road pavement construction [29]).

4.4. Rock properties

Fig. 9 represents the relation between rock bulk density (ρ_b) and uniaxial compression strength (UCS). The fitted line shows how the UCS increases with the ρ_b . In other words, the less porous the rock structure, the more resistant it will be.

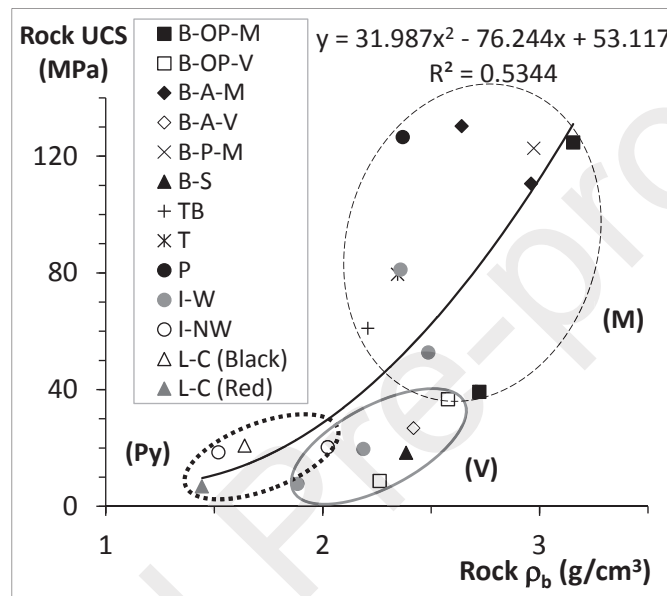


Fig. 9. Uniaxial compression strength (UCS) vs. bulk density (ρ_b) of the rock. (M) Massive lithotypes; (V) Vesicular lithotypes; (Py) Pyroclastic lithotypes.

Fig. 9 also shows the high dispersion of UCS values presented by the lithotypes with densities around 2.3-2.5 g/cm³. The variability observed seems to be related to various factors: rock structure, percentage of silica, and state of alteration. A vesicular structure offers less resistance compared to a massive structure due to the presence of voids that lead to cracking propagation and consequently to breaking. Generally, siliceous volcanic rocks tend to form a fine texture due to the high viscosity of magma, which results in fine-grained minerals with a large specific surface of bonding, and thus favouring high strength. However, chemical stability of volcanic rocks against alteration is not unequivocally determined by their chemical composition, but it is also related to the geologic age. A low alterability determines a higher rock resistance and stability in the medium and long term.

4.5. Relation between the properties of the volcanic aggregates and the matrix rock

Fig. 10 shows the relation between the intrinsic properties of the aggregate and the original rock. The aggregate particle density [dry] (ρ_{rd}) is a direct consequence of the rock bulk density (ρ_b). The function presents a reasonable setting ($R^2 = 0.76$), taking into account the dispersion of the results in the lower and mid part of the line. The dispersion for the lower densities is due to the heterogeneity of the pyroclasts (I-NW, L-C), the high void content (Fig. 4) and the mineralogical variability (salic, mafic). The dispersion in the mid-range of the function ($\rho_b \approx 2.3\text{--}2.5 \text{ g/cm}^3$) is related to the increase in porosity as the aggregate becomes smaller, at least in the case of coarse fractions (4-10 mm and 10-20 mm). This fact is a consequence of the increase of micro-cracking during the grinding process. The hypothesis is consistent with the petrographic observations of metamorphic aggregates in Ref. [36].

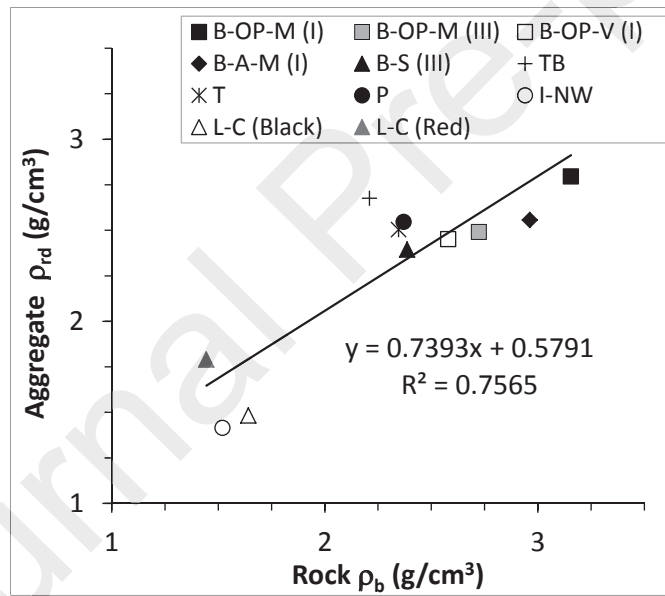


Fig. 10. Aggregate particle density [dry] (ρ_{rd}) vs. rock bulk density (ρ_b).

Fig. 11 shows the relation between the resistance to fragmentation of the aggregate and the rock strength. It relates the Los-Angeles coefficient (LA) of the aggregates with the uniaxial compression strength (UCS) of the matrix rock. The UCS value increases as the LA decreases, which results in a higher aggregate resistance. The fact that the two resistances (to fragmentation and to compression) show a direct correlation suggests that both depend on the same intrinsic property: density. Nevertheless, it must be taken into account that the load

applied during the LA test is multiple, dynamic and punctual and that in the uniaxial compression test a static and uniformly distributed load is applied. This observation suggests the existence of other determining properties such as the elastic modulus.

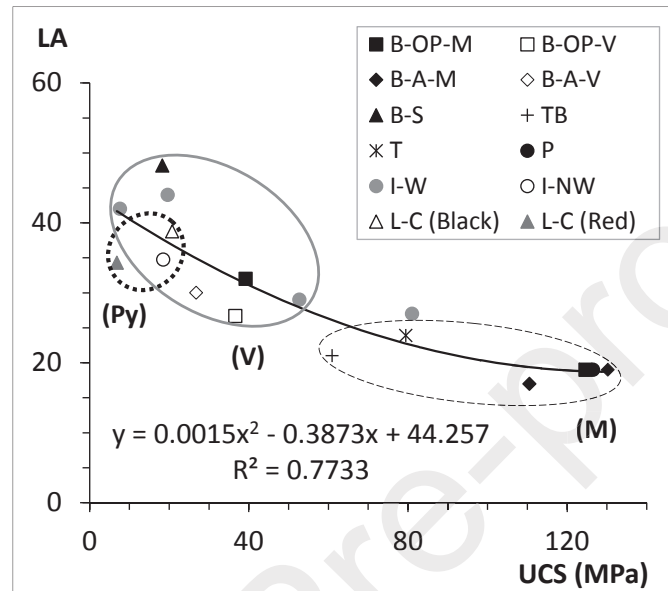


Fig. 11. Los-Angeles coefficient (LA) of the aggregate particles vs. uniaxial compression strength (UCS) of the source rock. (M) Massive lithotypes; (V) Vesicular lithotypes; (Py) Pyroclastic lithotypes.

5. CONCLUSIONS

From the analysis of the results of this experimental study the following conclusions may be drawn:

- Volcanic aggregates for engineering purposes may be classified for practical reasons in three extensive groups according to density, porosity (absorption) and resistance: massive, vesicular and pyroclastic. This simple classification allows users to take immediate decisions regarding possible construction applications depending on the volcanic aggregate available; and simplifying the much more complex geological classifications.

- The high statistical dispersion of the results shows the heterogeneity of the volcanic aggregates and in particular the pyroclasts. This variability is associated with both the geology and the production process of the aggregate. Among the geological factors the following are noteworthy: the geochemistry of the magma, the explosiveness of the volcanic eruptions and the random and discontinuous character of the spatial distribution of lava flows.
- The resistance of the volcanic aggregates is directly related to the mineralogy, porosity and grade of alteration of the source rock, and possibly with the elasticity modulus of the material. Furthermore, as the porosity increases so does the variability of the mechanical behaviour. This is particularly significant in the case of the pyroclasts.
- There is a relation between the intrinsic and mechanical properties of the original volcanic rock and the resulting aggregate. It is possible to estimate the aggregate LA coefficient from the rock UCS, as well as the aggregate particle density if the rock bulk density is known.
- The massive volcanic aggregates offer excellent resistance properties with high durability for road and airport paving, due to the high density and low porosity. However, certain lithotypes may present a flakiness index above the recommended limits established in the standard specifications.
- The vesicular and scoriaceous aggregates present high porosity associated with the high speed decompression and cooling of the lava flows. This determines a high absorption, rounded particle geometry with reduced percentage of crushed and broken surfaces, and susceptibility to weathering damage. For this reason, it would be advisable to limit their use to materials for base and subbase layers.
- The pyroclastic aggregates are only recommended for use as permeable subbases and subgrades, permeable low-weight fillings or in non-structural light concrete, due to the low density, high porosity and limited resistance to fragmentation although they offer excellent drainage capacity.

The use of local volcanic aggregates is a logistic and economic necessity especially in volcanic regions that are environmentally protected or in countries with limited technical and economic resources. Even the abundant vesicular and scoriaceous aggregates, generally considered marginal, can provide adequate quality

and performance for certain construction applications and therefore could contribute to the development of these areas and provide sustainable natural materials. For sustainable utilization of volcanic aggregates for cement concrete, additional chemical testing (stability, long-term durability) would be necessary.

Conflicts of interest

None.

Acknowledgements

This work was supported by the Ministry of Economy and Competitiveness (MINECO) from the Government of Spain, through the Research Project “MW-VolcAsphalt” (Ref. BIA2017-86253-C2-2-R, “Sustainable self-healable perpetual asphalt pavements with volcanic aggregates using microwaves and additions of metallic wastes and nanoparticles”).

The authors are also very grateful to the Construction Laboratory of the Government of Canary Islands (J. Jubera and J. Santana) for accessing to the quality control test reports and to all the students who have collaborated with enthusiasm in the laboratory tests (P. Pérez-Velarde, J. Soto, C. Alonso, A. Santana, T. Armas, J. Catalá, and a long etc.).

References

- [1] Akbulut H, Güner C, Çetin S (2011). *Use of volcanic aggregates in asphalt pavement mixes*. In: Proceedings of the institution of Civil Engineers. Transport, 164 (TR2): 111-123. <https://doi.org/10.1680/tran.2011.164.2.111>
- [2] Franesqui MA, Yepes J, García-González C (2019). *Improvement of moisture damage resistance and permanent deformation performance of asphalt mixtures with marginal porous volcanic aggregates using crumb rubber modified bitumen*. Construction and Building Materials, 201: 328–339. <https://doi.org/10.1016/j.conbuildmat.2018.12.181>
- [3] Al-Khateeb GG, Khedaywi TS, Obaidat TIA, Najib AM (2013). *Laboratory Study for Comparing Rutting Performance of Limestone and Basalt Superpave Asphalt Mixtures*. Journal of Material in Civil Engineering, 25: 21-9. [https://doi.org/10.1061/\(ASCE\)MT.1943-5533.0000519](https://doi.org/10.1061/(ASCE)MT.1943-5533.0000519)

- [4] Behiry A (2016). *Optimisation of hot mix asphalt performance based on aggregate selection*. International Journal of Pavement Engineering, 10: 924-940. <https://doi.org/10.1080/10298436.2015.1043634>
- [5] Franesqui MA, Castelo-Branco F, Azevedo MC, Moita P (2010). *Construction experiences with volcanic unbound aggregates in road pavements*, in: Volcanic Rock Mechanics, Olalla et al. (Eds.), Taylor & Francis Group, London (2010) 241-247. <http://www.crcnetbase.com/doi/abs/10.1201/b10549-36>
- [6] Török, Á (2015). *Los-Angeles and Micro-Deval values of volcanic rocks and their use as aggregates, examples from Hungary*. In: Engineering Geology for Society and Territory - Volume 5. Urban Geology, Sustainable Planning and Landscape Exploitation: 115-118. https://doi.org/10.1007/978-3-319-09048-1_23
- [7] Bogas JA, Gomes T (2015). *Mechanical and durability behaviour of structural lightweight concrete produced with volcanic scoria*. Arabian Journal for Science and Engineering, 40: 705-717. <https://doi.org/10.1007/s13369-014-1550-4>
- [8] Cai G, Noguchi T, Degee H, Zhao J and Kitagaki R (2016). *Volcano-related materials in concretes: a comprehensive review*. Environmental Science and Pollution Research, 23 (8): 7220-7243. <https://doi.org/10.1007/s11356-016-6161-z>
- [9] Juimo W, Cherradi T, Abidi L and Oliveira L (2016). *Characterisation of Natural Pozzolan of "Djounjo" (Cameroon) as Lightweight Aggregate for Lightweight Concrete*. International Journal of Geomate, 11 (27): 2782-2789. <https://doi.org/10.21660/2016.27.1310>
- [10] Lomoschitz A, Jimenez JR, Yepes J, Perez-Luzardo JM, Macias-Machin A, Socorro M, Hernandez, LE, Rodriguez JA, Olalla C (2006). *Basaltic lapilli used for construction purposes in the Canary Islands, Spain*. Environmental & Engineering Geoscience, 12 (4): 327-336. <https://doi.org/10.2113/gseegeosci.12.4.327>
- [11] Szilagyi H, Baera C, Corbu O, Puskas A (2016). *Research and Valorization of Volcanic Tuff Aggregates in Lightweight Concrete*. Nano, Bio and Green - Technologies for a Sustainable Future Conference Proceedings, Sgem 2016, Vol II: 197-202. <https://doi.org/10.5593/SGEM2016/B62/S26.027>
- [12] Aghamelu OP, Okogbue CO (2015). *Usability of pyroclastic rocks as construction materials; example from Nigeria*. Engineering Geology for Society and Territory - Volume 5: Urban Geology, Sustainable Planning and Landscape Exploitation: 1259-1262. https://doi.org/10.1007/978-3-319-09048-1_240

- [13] Naji, JA, Asi IM (2008). *Performance evaluation of asphalt concrete mixes containing granular volcanic ash*. Journal of Materials in Civil Engineering, 20 (12): 754-761. [https://doi.org/10.1061/\(ASCE\)0899-1561\(2008\)20:12\(754\)](https://doi.org/10.1061/(ASCE)0899-1561(2008)20:12(754))
- [14] Okogbue CO, Aghamelu OP (2013). *Performance of pyroclastic rocks from Abakaliki Metropolis (southeastern Nigeria) in road construction project*. Bulletin of Engineering Geology and the Environment, 72 (3-4): 433-446. <https://doi.org/10.1007/s10064-013-0489-0>
- [15] Smith, M.R. Collis, L. (1993). *Aggregates: sand, gravel and crushed rocks for construction purposes*. The Geological Society, London.
- [16] Abo-Qudais S, Al-Shweily H (2007). *Effect of aggregate properties on asphalt mixtures stripping and creep behavior*. Construction and Building Materials, 9: 1886-1898. <https://doi.org/10.1016/j.conbuildmat.2005.07.014>
- [17] Krutilova K and Prikryl R (2017). *Relationship between polished stone value (PSV) and Nordic abrasion value (A (N)) of volcanic rocks*. Bulletin of Engineering Geology and the Environment, 76 (1): 85-99. <https://doi.org/10.1007/s10064-015-0814-x>
- [18] Ugur I, Demirdag S, Yavuz H (2010). *Effect of rock properties on the Los-Angeles abrasion and impact test characteristics of the aggregates*. Materials characterization, 61 (1): 90-96. <https://doi.org/10.1016/j.matchar.2009.10.014>
- [19] Hernández-Gutiérrez LE, Rodríguez-Losada JA, Hernández-Fernández S (2008). *Resistance to fragmentation of volcanic rocks as aggregates in concrete and asphalt*. Geo-Temas, 10: 887-890.
- [20] Kahraman S, Delibalta MS, Comakli R, Grafov BM (2013). *Noise level measurement test to predict the abrasion resistance of rock aggregates*. Fluctuation and Noise Letters, 12 (4), art. 135002. <https://doi.org/10.1142/S0219477513500211>
- [21] Kahraman S, Fener M (2008). *Electrical resistivity measurements to predict abrasion resistance of rock aggregates*. Bulletin of Materials Science, 31 (2): 179-184. <https://doi.org/10.1007/s12034-008-0031-3>
- [22] Kahraman S, Gunaydin O. (2007). *Empirical methods to predict the abrasion resistance of rock aggregates*. Bulletin of Engineering Geology and the Environment, 66 (4): 449-455. <https://doi.org/10.1007/s10064-007-0093-2>
- [23] Aparicio A., Hernán F, Cubas CR, Araña V (2003). *Fuentes mantélicas y evolución del volcanismo canario*. Estudios Geológicos, 59 (1-4): 5-14 (in Spanish).
- [24] Bryan SE, Marti J, Cas RAF (1998). *Stratigraphy of the Bandas del Sur Formation: an extracaldera record of Quaternary phonolitic explosive eruptions from the Las Cañadas edifice, Tenerife (Canary Islands)*. Geological Magazine 135 (5): 605-636.

- [25] Rodríguez-Losada JA, Hernandez-Gutierrez LE, Lomsochitz A (2007). *Geotechnical features of the welded ignimbrites of the Canary Islands*. In: Proceedings of the International Workshop on Volcanic Rocks, Workshop W2 - 11th Congress ISRM. <https://doi.org/10.1201/NOE0415451406.ch4>
- [26] Rodríguez-Losada JA, Hernandez-Gutierrez LE, Olalla C, Perucho A, Serrano A, del Potro R (2007). *The volcanic rocks of the Canary Islands. Geotechnical properties*. In: Proceedings of the International Workshop on Volcanic Rocks, Workshop W2 - 11th Congress ISRM: 53-57. <https://doi.org/10.13140/2.1.2770.9444>
- [27] Rodríguez-Losada JA, Hernandez-Gutierrez LE, Olalla C, Perucho A, Serrano A, Eff-Darwich A (2009). *Geomechanical parameters of intact rocks and rock masses from the Canary Islands: Implications on their flank stability*. Journal of Volcanology and Geothermal Research, 182 (1-2): 67-75. <https://doi.org/10.1016/j.jvolgeores.2009.01.032>
- [28] Canary Islands Regional Government (2011). *Guide for Geotechnical Studies in Building in the Canary Islands*. GETCAN-011 (in Spanish).
- [29] Spanish Ministry of Infrastructures (2014). *Spanish General Technical Specifications for Roads and Bridges* (PG-3, Art. 542 & 543). Orden FOM/2523/2014. Madrid, Spain, 2014 (in Spanish).
- [30] US Department of Transportation. Federal Highway Administration (2014). *Standard Specifications for Construction of Roads and Bridges on Federal Highway Projects* (FP-14) (Section 703. Aggregate).
- [31] UK Highways Agency (2019). *Manual of Contract Documents for Highway Works* (MCHW). (Volume 1-Specifications for Highway Works. Series 900. Road Pavements – Bituminous Bound Materials). Amendment – July 2019.
- [32] International Society of Rock Mechanics ISRM (1981). *Suggested methods for rock characterization, testing and monitoring*. Oxford: E.T. Brown. Pergamon Press.
- [33] Vergnolle S, Mangan M (2000). *Hawaiian and strombolian eruptions*. in: Encyclopedia of Volcanoes (eds. H. Sigurdsson, B. Houghton, S. McNutt, H. Rymer, J. Stix) Academic Press, 447-461.
- [34] Kamani M, Ajalloeian R (2020). *The effect of rock crusher and rock type on the aggregate shape*. Construction and Building Materials, 230: 117016. <https://doi.org/10.1016/j.conbuildmat.2019.117016>
- [35] Khaleghi Esfahani M, Kamani M, Ajalloeian R (2019). *An investigation of the general relationships between abrasion resistance of aggregates and rock aggregate properties*. Bulletin of Engineering Geology and the Environment, 78: 3959-3968. <https://doi.org/10.1007/s10064-018-1366-7>

[36] Pérez-Fortes AP, Varas-Muriel MJ, Castiñeiras P (2017). *Using petrographic techniques to evaluate the induced effects of NaCl, extreme climatic conditions, and traffic load on Spanish road surfaces*. *Materiales de Construcción*, 67 (328): 1-11. <http://dx.doi.org/10.3989/mc.2017.07516>

Declaration of interests

☒ The authors declare that they have no known competing financial interests or personal relationships that could have appeared to influence the work reported in this paper.

☐ The authors declare the following financial interests/personal relationships which may be considered as potential competing interests:

[37]

AUTHORS DECLARATION

We wish to confirm that there are no known conflicts of interest associated with this publication and there has been no significant financial support for this work that could have influenced its outcome.

We confirm that the manuscript has been read and approved by all named authors and that there are no other persons who satisfied the criteria for authorship but are not listed. We further confirm that the order of authors listed in the manuscript has been approved by all of us.

We confirm that we have given due consideration to the protection of intellectual property associated with this work and that there are no impediments to publication, including the timing of publication, with respect to intellectual property. In so doing we confirm that we have followed the regulations of our institutions concerning intellectual property.